SUPPLEMENTARY METHODS

Deep-time phylogeographic analyses

Approximate Bayesian Computation

Analyses of *Araptus attenuatus* mt*COI* data inferred a phylogenetic tree topology in which major Clades C and S are sisters, and Clade B is early-branching (Fig. 3 in the main text; also supported by DIY-ABC analyses in Fig. S2). Two alternative divergence histories that may have generated this topology where investigated further. The first scenario involves a single colonization of continental Sonora (where Clade S now resides) sourced from the Baja peninsula (i.e., the ancestor of Clade C), with a concomitant bottleneck of the Clade S lineage that occurred during long-distance overwater dispersal. The competing scenario involves two independent and temporally spaced colonizations of the Baja peninsula (with Clade B arrival postdating that of Clade C) from a continental ancestor. Again, each long-distance overwater dispersal event was assumed to be associated with a bottleneck.

DIY-ABC v1.0.4.46b (Cornuet *et al*. 2010) was used to distinguish among the alternative scenarios, and closely followed the procedure used when reassessing relationships among major mt*COI* clades (see main text Methods). In this case, two additional parameters were used to characterize a bottleneck, both with uniform priors: *duration*, which is number of number of generations for which N_e remained low (*Dur.* = 10–1000), and *severity*, which is the actual N_e during the bottleneck (*Sev.* = 10–1000, equivalent to at least a 99% reduction in size). Both

competing models included the same two bottleneck parameters, with all other model parameters and priors the same as those previously used (see main text Methods). Thus, despite representing one- *vs*. two-event colonization scenarios, overall model complexity was equivalent. The same set of seven single-sample summary statistics given in the main text Methods was also used here. DIY-ABC runs consisted of 3.0×10^6 simulations (1.5×10^6 per demographic scenario). Model checking, posterior probabilities of scenarios, and estimates of parameters of best-fit model where performed following Cornuet *et al*. (2010).

Shallow-time phylogeographic analyses

Coalescent simulations

Reconciliation of gene tree *vs*. population tree discordance, and statistical discrimination among alternative scenarios, can be facilitated by coalescent modeling (Knowles 2004). We used simulations to determine whether incomplete lineage sorting was a plausible explanation for the lack of strong mt*COI* phylogeographic structure among three allopatric regional populations (NBP, CBP and SBP) with spatial-genetic boundaries that roughly correspond with Riddle *et al*.'s (2000) predictions relating to ancient vicariance events (Figs. 1 and 4 in the main text). We tested the proposed timescales of Plio- and/or Pleistocene-aged marine inundations (i.e., mid-peninsular seaway, 1 MYA; Isthmus of La Paz, 3 MYA; and a composite 'two-tiered vicariance' scenario including both events). These three scenarios have previously been tested in *E. lomelii* (Garrick *et al.* 2009). We also examined the possibility of more recent divergence at the height of the Last Glacial Maximum (LGM scenario, 18 KYA; Fig. S6).

Divergence scenarios were represented as population trees, summarized by bifurcations (vicariance events), branch lengths (time since splitting) and branch widths (effective population sizes, N_e; see Fig. S6). To set N_e of extant regional populations, we first estimated theta ($\Theta = N_e\mu$ for mt*COI*, where μ is the per-site per-generation mutation rate) using FLUCTUATE v1.4 (Kuhner *et al.* 1998). Search settings were 10 short MCMC chains (10^4 steps), five long chains (10^5 steps) sampling every 20^{th} genealogy, random starting trees, empirical ts/tv ratio and base frequencies, starting Θ-value from Watterson's estimate, and no growth. The mean Θ-value from five runs was accepted (Table S3). To convert Θ to N_e, we assumed three generations per year based on related bark beetles from similar climates (Dreistadt *et al.* 2004) and applied Brower's (1994) standard arthropod mtDNA substitution rate. Branch widths at internal nodes (ancestral populations) were set by summing N_e of the descendant populations. For computational tractability, we rescaled N_e-values and generations since splitting (all divided by 100).

The simplifying assumption of no post-divergence long-distance dispersal is unlikely to hold for *A. attenuatus* owing to the potential for flight. Accordingly, we explored the impacts on phylogeographic inference of incorporating migration into the coalescent simulations.
For each scenario, coalescent mt*COI* gene trees were simulated within the constraints of each population tree using empirical sample sizes of regional populations previously identified from genotypic clustering using STRUCTURE (Fig. S6). Simulated datasets were generated assuming either zero post-divergence migration, or continuous migration (probability of migration/individual/generation, $P_{MIG} = 1x10^{-4}$, $1x10^{-5}$ or $1x10^{-6}$; 500 replicates each). DNA

characters (403-bp) were simulated using the GTR+I+G substitution model and scenario-specific scaling factors that approximated empirical mt*COI* polymorphism levels (Fig. S6). Neighbor-joining (NJ) gene trees were estimated in PAUP* v4.0b10 (Swofford 2002) using maximum-likelihood corrected distances with model and parameters from MODELTEST. Maddison's (1997) Deep Coalescences (*DC*), was calculated for each unrooted NJ tree in MESQUITE v2.5 (Maddison & Maddison 2008). Significance was assessed via comparison of distributions of *DC*-values simulated with or without migration versus empirical *DC*-values ($\alpha = 0.05$, two-tailed test). Significantly large *DC* indicates a younger population splitting time than predicted by incomplete lineage sorting, whereas significantly small values suggest older splitting times.

SUPPLEMENTARY TABLES

Table S1. Bioclimatic layers contributing (≥ 5%) to the estimated Ecological Niche Model in terms of the percent to the estimated model and permutation importance.

Bioclimatic Variable	**Contribution**	**Importance**
Mean Diurnal Temperature Range (BIO2)	27.2	2.3
Annual Temperature Range (BIO7)	13.7	2.4
Precipitation Seasonality (BIO15)	13.2	16.2
Driest Quarter Precipitation (BIO17)	8.6	7.8
Mean Temperature Wettest Quarter (BIO8)	7.9	13.4
Wettest Month Precipitation (BIO13)	7.0	12.7

Table S2. Tests of population growth within Clade B (Baja) based on the frequency distribution of mt*COI* haplotypes. Regional population abbreviations follow Fig. 4 in the main text. The number of individuals sequenced (N_{mtCOI}) and number of unique haplotypes resolved ($N_{Haplotypes}$) are shown, and F_S is the observed value (note that some haplotypes are shared among the three regional populations). Where $N_{mtCOI} < 50$, the null hypothesis of no growth was re-assessed using R_2 (SBP: $R_2 = 0.148$, P = ns, not shown). P-value is the probability that the observed test statistic is significantly small, at the 0.02 level (ns = not significant).

Regional population	N_{mtCOI}	$N_{Haplotypes}$	F_S	P-value
NBP	63	15	-3.1083	ns
CBP	124	43	-28.0329	<0.0001
SBP	12	8	0.7616	ns

Table S3. Estimates of Θ for *Araptus attenuatus* regional populations used in coalescence-with-migration simulations (abbreviations follow Fig. 4 in the main text). Empirical mt*COI* sample sizes (N_{mtCOI}) were used in the simulations. Mean and standard deviation of Θ-values were calculated from five independent FLUCTUATE runs.

Vicariance scenario	Regional population(s)	N_{mtCOI}	Mean Θ	(Std. Dev.)
Last Glacial Maximum	NBP	63	0.0170	(0.0007)
	CBP	124	0.0495	(0.0005)
	SBP	12	0.0360	(0.0005)
Mid-peninsular seaway	NBP	63	0.0170	(0.0007)
	CBP+SBP	136	0.0623	(0.0018)
Isthmus of La Paz	NBP+CBP	187	0.0544	(0.0013)
	SBP	12	0.0360	(0.0005)
Two-tiered vicariance	NBP	63	0.0170	(0.0007)
	CBP	124	0.0495	(0.0005)
	SBP	12	0.0360	(0.0005)

SUPPLEMENTARY FIGURES

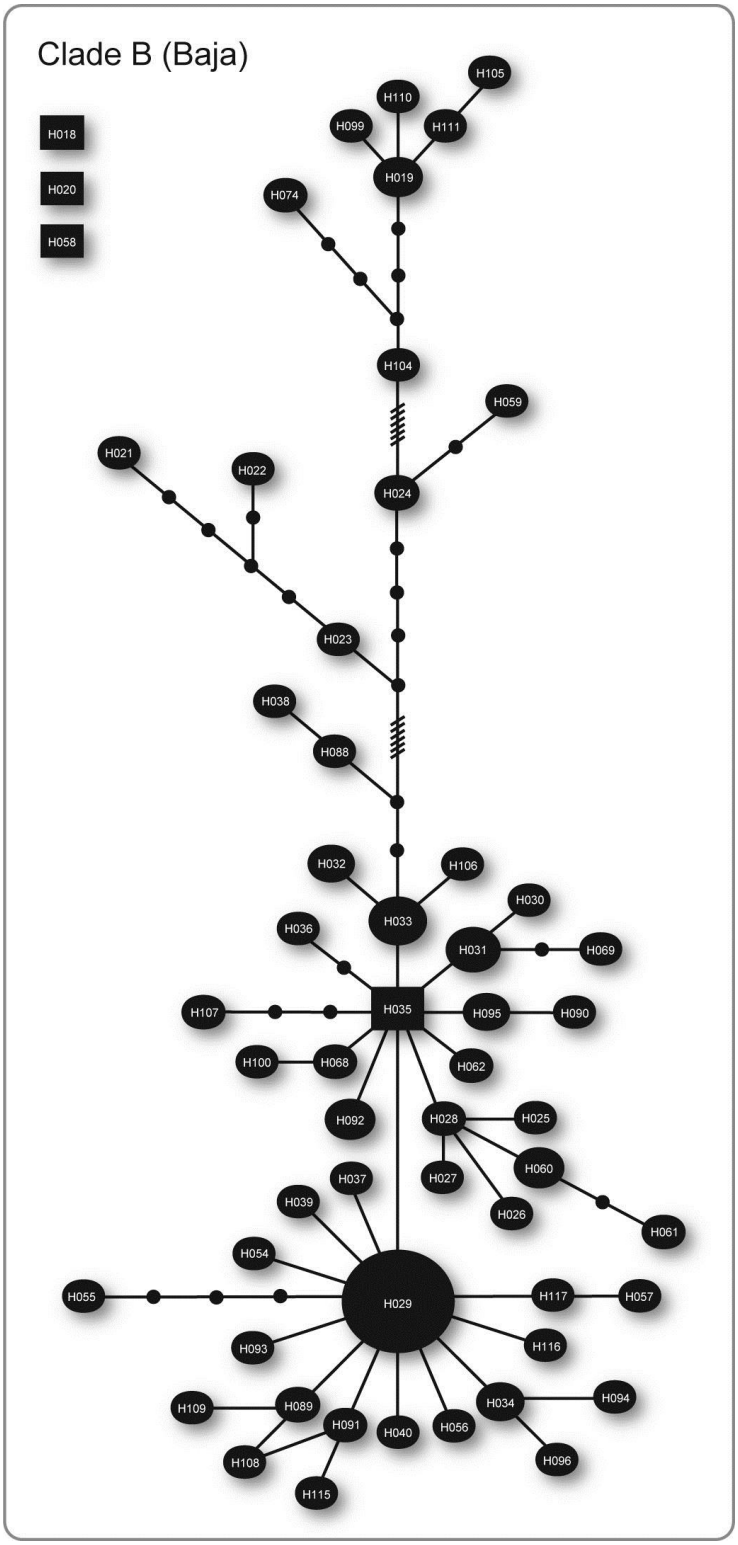

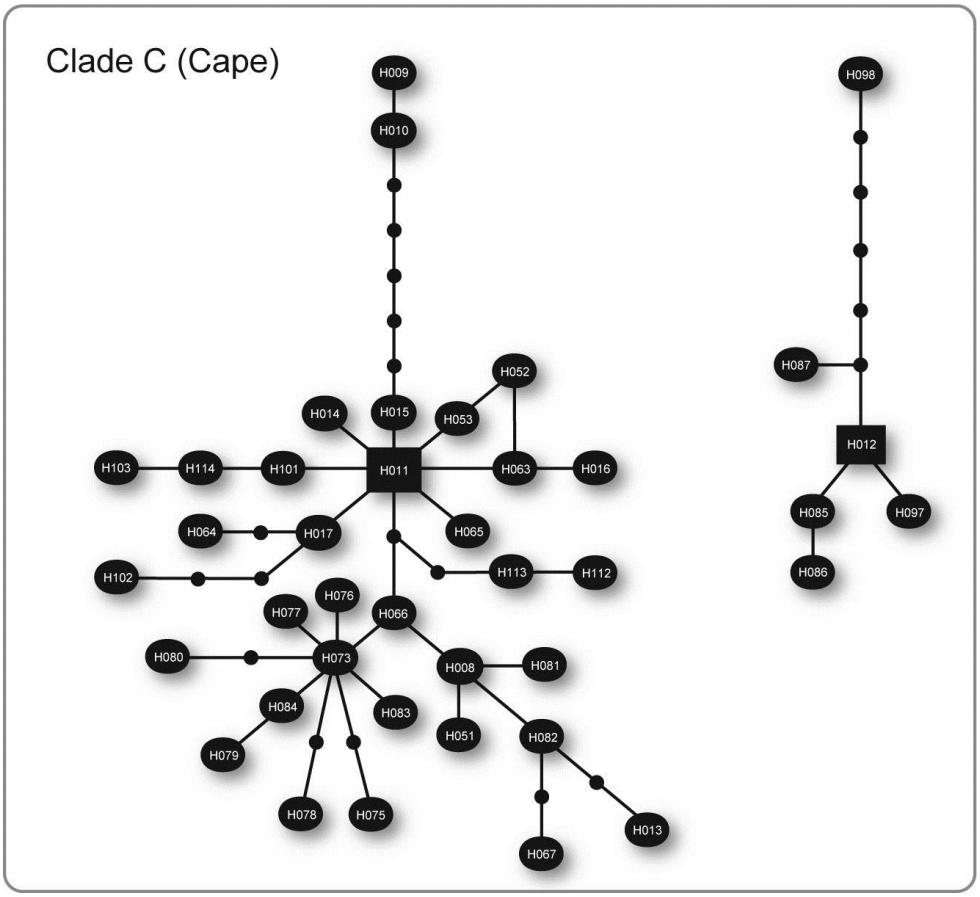
Clade C (Cape)
H009
H010
H052
H014
H015
H053
H103
H114
H101
H011
H063
H016
H064
H017
H065
H102
H113
H112
H076
H077
H066
H080
H073
H008
H081
H084
H083
H051
H082
H079
H078
H075
H013
H067
H098
H087
H012
H085
H097
H086

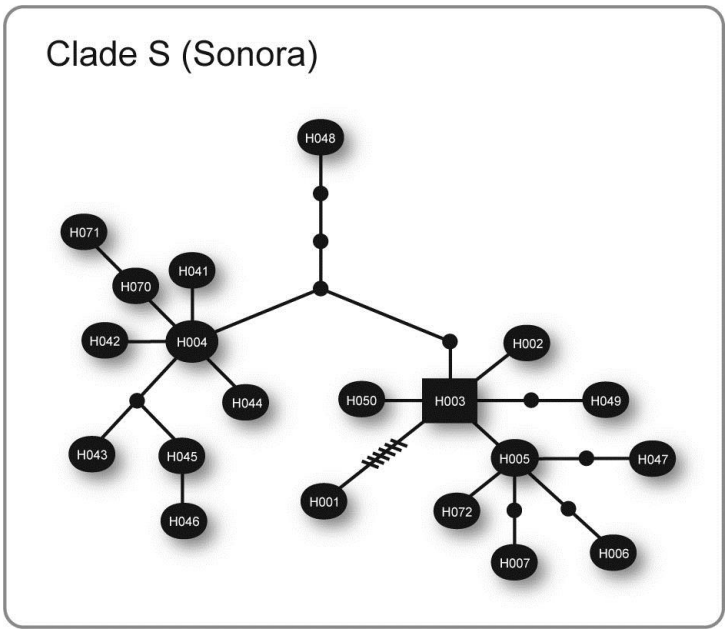

Figure S1. Relationships among mitochondrial DNA haplotypes estimated using Statistical Parsimony in TCS v. 1.21 (Clement *et al* 2000). Each black oval is a different haplotype (labeled following Fig. 3 of the main text). The size of each oval is proportional to frequency of that haplotype. Single black lines represent one mutational step, and small black circles represent inferred haplotypes that were not sampled or are extinct. A series a crossbars indicate a set of seven mutational steps. Disconnected networks were formed when the 95% confidence connection limit (8 steps) was exceeded. Within each network, a rectangle indicates the haplotype with the highest outgroup weighting. Where possible, reticulations were resolved following Pfenninger & Posada (2002).

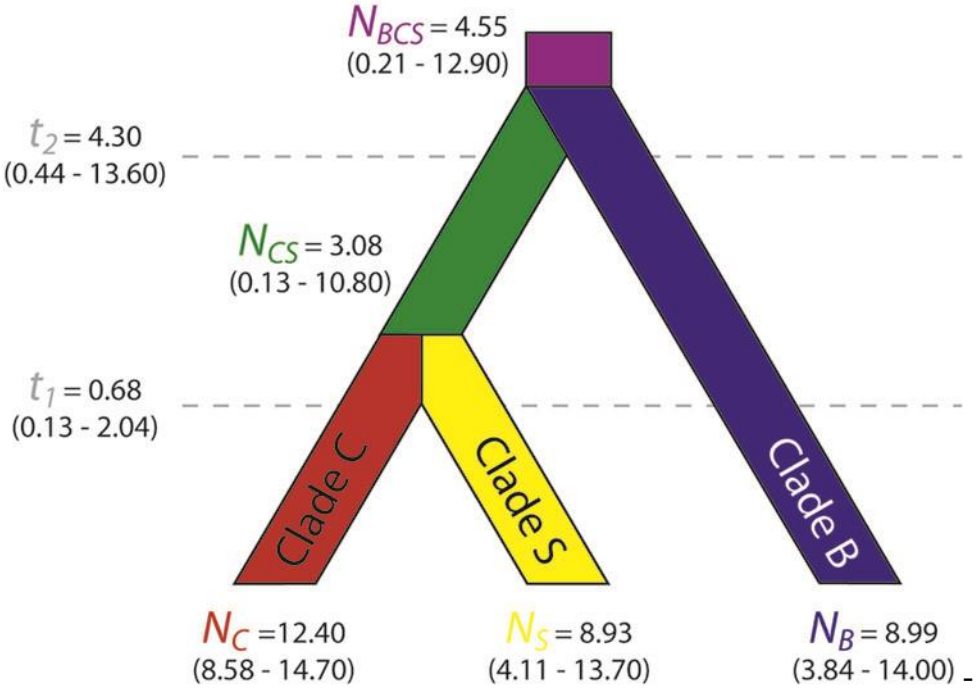

Figure S2. Best-fit model of evolutionary relationships among populations in which major mt*COI* clades evolved (Clade B, Baja; Clade C, Cape Region; Clade S, Sonora), estimated using DIY-ABC. Point estimates (mean values) and 90% confidence intervals are shown. Model parameters are as follows: *N* = effective population size (in units of 10^6), where subscripts indicate contemporary major clade ($_B$, $_C$ or $_S$) or ancestral lineage; and *t* = splitting time in MYA, where subscripts indicate youngest *vs*. oldest split ($_1$ and $_2$, respectively).

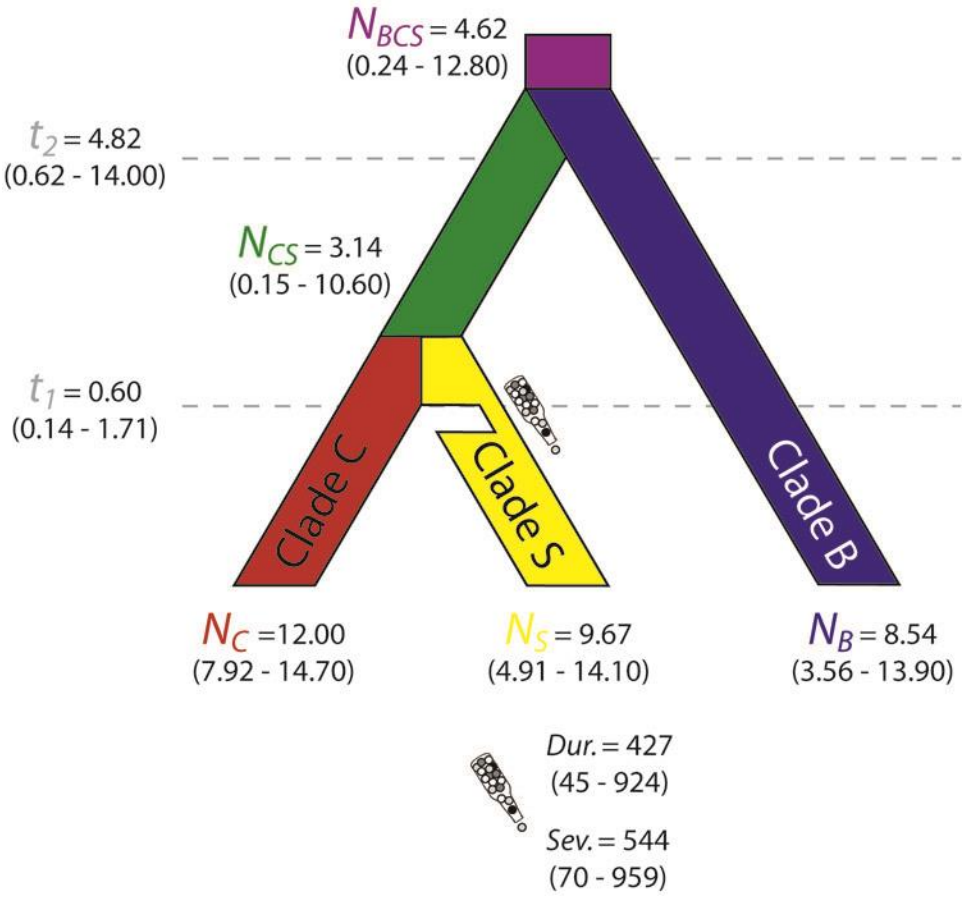

Figure S3. Best-fit model of colonization history of populations in which major mt*COI* clades evolved (Clade B, Baja; Clade C, Cape Region; Clade S, Sonora), estimated using DIY-ABC. Point estimates (mean values) and 90% confidence intervals are shown. Model parameters are as follows: N = effective population size (in units of 10^6), where subscripts indicate contemporary major clade ($_B$, $_C$ or $_S$) or ancestral lineage; and t = splitting time in MYA, where subscripts indicate youngest *vs*. oldest split ($_1$ and $_2$, respectively). The bottleneck event associated with long-distance over-water colonization of continental Sonora (Clade B) from a Baja peninsula ancestor is characterized by *duration* (*Dur.*) and *severity* (*Sev.*); these are not scaled by 10^6, but rather, are presented as raw values (in units of generations and N_e, respectively).

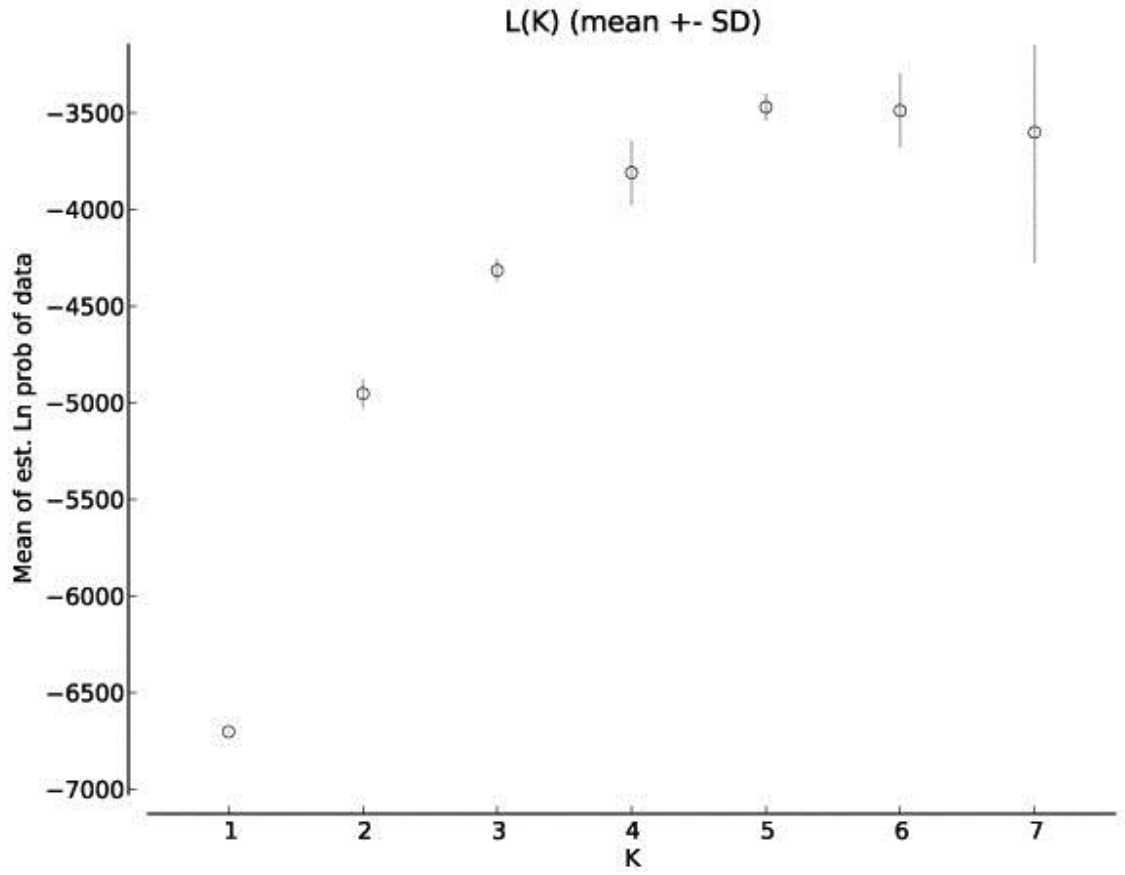

Figure S4. Plot of the number of clusters (*K*; *x*-axis) versus negative log likelihood (-ln L) of the data (*y*-axis), based on four replicate runs per *K* using STRUCTURE. The smallest 'best-fit' value of $K = 4$ was chosen following Pritchard *et al*. (2000), and validated using the method of Evanno *et al*. (2005; not shown). Additional support for $K = 4$ comes from Ecological Niche Modeling, and geographic cohesiveness of inferred clusters (Figs. 2 and 4 in the main text, respectively).

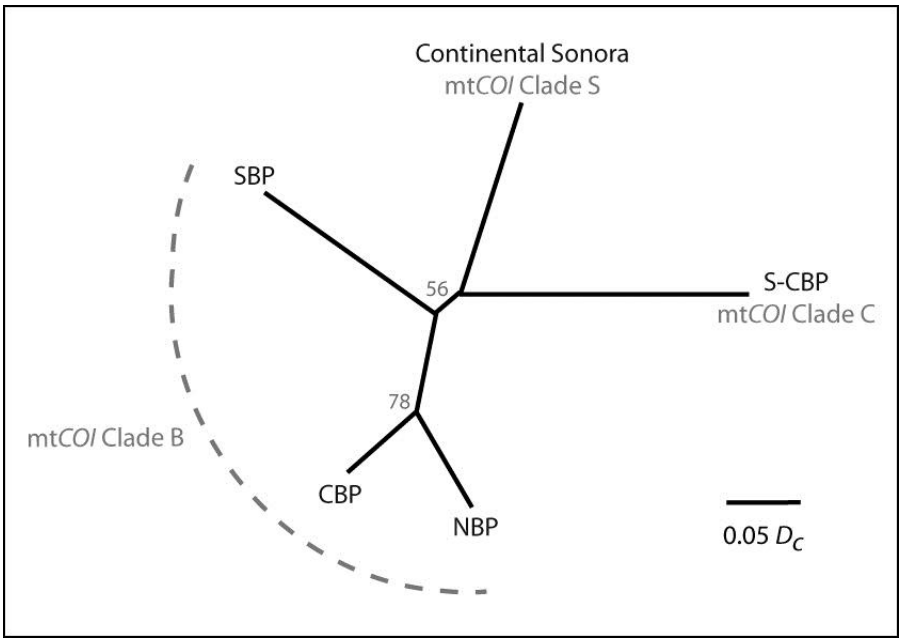

Figure S5. Neighbor-joining tree showing relationships among regional populations based on nuclear allele frequencies (chord distance, *Dc*). Abbreviations follow Fig. 4 in the main text, with mt*COI* major clade membership labeled. Numbers at nodes indicate bootstrap support >50% (1,000 replicates).

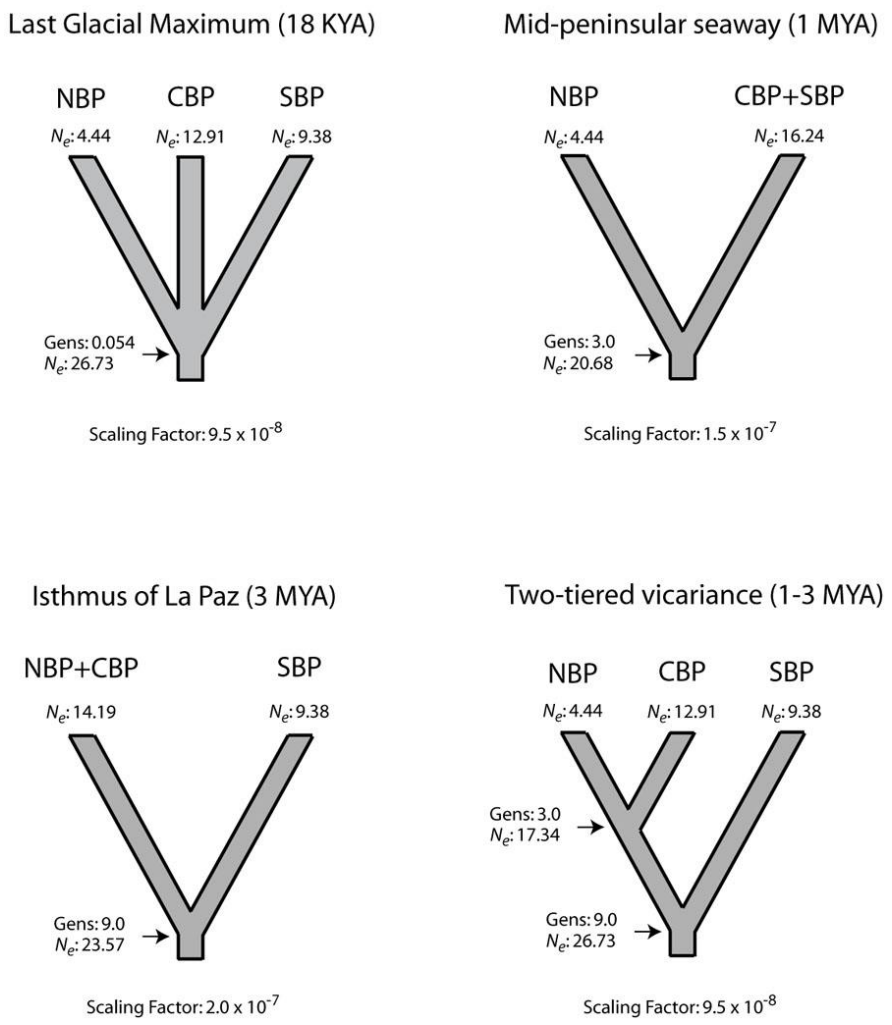

Figure S6. Model parameters of alternative vicariance scenarios tested using mt*COI* sequence data from *Araptus attenuatus*. Regional population abbreviations follow Fig. 4 in the main text. Effective population sizes (N_e) are given in units of 10^6. For extant populations (i.e., tips on the tree), N_e-values were calculated using Θ-values given in Table S3 using Brower's (1994) standard arthropod mtDNA rate (assuming three generations/year). Effective population sizes of internal nodes are the sum of descendent population N_e-values. 'Gens' represents the number of organismal generations since a hypothesized splitting event, also given in units of 10^6.

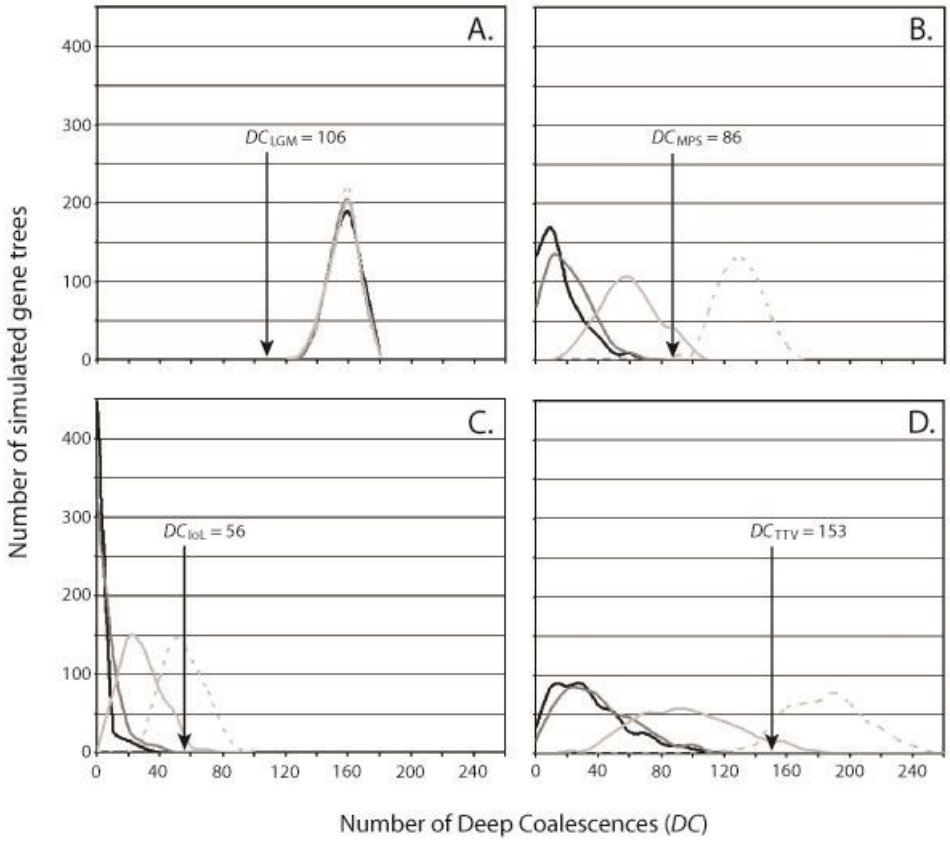

Figure S7. Coalescence-with-migration tests of four alternative Baja peninsula vicariance scenarios: (A) Last Glacial Maximum, LGM, (B) mid-peninsular seaway, MPS, (C) Isthmus of La Paz, IoL, and (D) two-tiered vicariance, TTV. Null distributions of the test-statistic (number of Deep Coalescences, *DC*) were generated by simulating DNA sequence datasets within the constraints of each *a priori* scenario (see Fig. S6) using one of four per-generation migration probabilities: zero (black solid lines), 10^{-6} (dark gray solid lines), 10^{-5} (pale gray solid lines), and 10^{-4} (pale gray dashed lines). *DC*-values calculated from the empirical mt*COI* dataset are shown by arrows, and *P*-values for each hypothesis test are given in Table 1 of the main text.

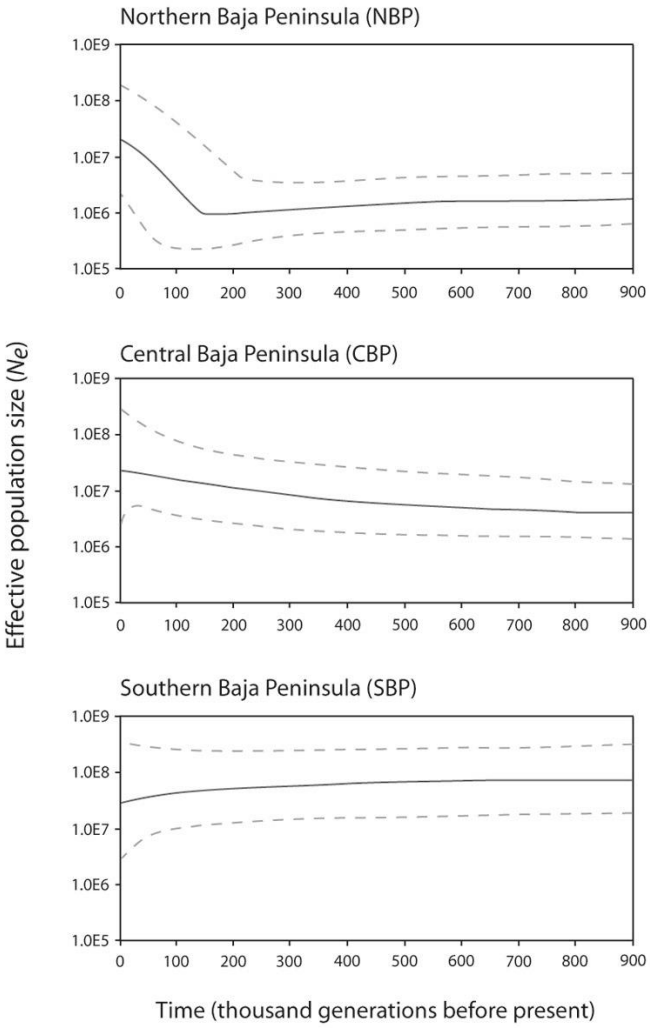

Figure S8. Bayesian skyline plots showing population sizes changes over time, estimated using BEAST. Mitochondrial *COI* sequence datasets from regional populations NBP, CBP and SBP were analyzed (sample sizes follow Table S2). The *y*-axis shows absolute effective population size (N_e) on a logarithmic scale, assuming used Brower's (1994) standard arthropod mtDNA rate (assuming three generations/year). In each skyline plot, a dark solid line represents the median estimate of N_e over time, and dashed gray lines show the 95% highest posterior density limits.

SUPPLEMENTARY REFERENCES

Brower AVZ (1994) Rapid morphological radiation and convergence among races of the butterfly *Heliconius erato* inferred from patterns of mitochondrial DNA evolution. *Proceedings of the National Academy of Sciences, USA*, **91**, 6491–6495.

Clement M, Posada D, Crandall KA (2000) TCS: A computer program to estimate gene genealogies. *Molecular Ecology*, **9**, 1657–1659.

Cornuet J-M, Ravigné V, Estoup A (2010) Inference on population history and model checking using DNA sequence and microsatellite data with the software DIYABC (v1.0). *BMC Bioinformatics*, **11**, 401.

Dreistadt SH, Dahlsten DL, Paine TD (2004) Bark beetles: integrated pest management for home gardeners and landscape professionals. In: *Pest Notes* (ed. Flint ML), publication 7421, pp. 1–4. University of California, Davis, CA. www.ipm.ucdavis.edu

Evanno, G, Regnaut S, Goudet J (2005) Detecting the number of clusters of individuals using the software STRUCTURE: A simulation study. *Molecular Ecology*, **14**, 2611–2620.

Garrick RC, Nason JD, Meadows CA, Dyer RJ (2009) Not just vicariance: Phylogeography of a Sonoran Desert euphorb indicates a major role of range expansion along the Baja peninsula. *Molecular Ecology*, **18**, 1916–1931.

Knowles LL (2004) The burgeoning field of statistical phylogeography. *Journal of Evolutionary Biology*, **17**, 1–10.

Kuhner MK, Yamato J, Felsenstein J (1998) Maximum likelihood estimation of population growth rates based on the coalescent. *Genetics*, **149**, 429–434.

Maddison W (1997) Gene trees in species trees. *Systematic Biology*, **46**, 523–536.

Maddison WP, Maddison DR (2008) Mesquite: a modular system for evolutionary analysis. Version 2.5. http://mesquiteproject.org

Pfenninger M, Posada D (2002) Phylogeographic history of the land snail *Candidula unifasciata* (Helicellinae, Stylommatophora): Fragmentation, corridor migration, and secondary contact. *Evolution*, **56**, 1776–1788.

Pritchard JK, Stevens M, Donnelly P (2000) Inference of population structure using multilocus genotype data. *Genetics*, **155**, 945–959.

Riddle BR, Hafner DJ, Alexander LF, Jaeger JR (2000) Cryptic vicariance in the historical assembly of a Baja California Peninsular Desert biota. *Proceedings of the National Academy of Sciences, USA*, **97**, 14438–14443.

Swofford DL (2002) PAUP*: Phylogenetic analysis using parsimony (* and other methods). Sinauer, Sunderland, MA.